

ОБЪЕДИНЕННЫЙ
ИНСТИТУТ
ЯДЕРНЫХ
ИССЛЕДОВАНИЙ

Дубна

DD

E13-96-358
MPI-PhE/96-15

RADIATION HARDNESS OF GaAs PREAMPLIFIERS
FOR LIQUID ARGON CALORIMETRY AT LHC

Submitted to «Nuclear Instruments and Methods A»

SCAN-9704105



CERN LIBRARIES, GENEVA

swy716

1996

A.Cheplakov, V.Golikov, S.Golubiyh, V.Kukhtin, E.Kulagin, E.Ladygin,
V.Luschikov, R.Mehdiyev¹, V.Obudovsky, D.Salihagic², E.Shabalin,
A.Shalyugin, G.Yarygin

Joint Institute for Nuclear Research, Dubna

J.Ban³, V.Bartheld, H.Brettel, J.Fent, K.Jakobs⁴, H.Oberlack,
A.Osthoff, P.Schacht, U.Stiegler⁵, T.Zweimüller
Max-Planck-Institut für Physik, München, Germany

¹Permanent address: Institute of Physics, Baku, Azerbaijan

²Permanent address: Montenegro University, Podgorica, Montenegro

³Permanent address: Institute of Experimental Physics, Košice, Slovak Republic

⁴Now at Institut für Physik, Universität Mainz, Germany

⁵Now at CERN, 1211 Geneva, Switzerland

1 Introduction

Many components of the front-end electronics of the ATLAS detector at LHC will be located in the high radiation field of photons and neutrons expected at the high luminosity running. One example are the preamplifiers immersed in the cryostat of the hadronic liquid argon end-cap calorimeter. At the expected high luminosity of $\mathcal{L} = 1.0 \cdot 10^{34} \text{ cm}^{-2}\text{s}^{-1}$ a maximum yearly dose of 12 kGy yr^{-1} and a 1 MeV equivalent neutron fluence of $1.0 \cdot 10^{15} \text{ n cm}^{-2} \text{ yr}^{-1}$ are expected in the hadronic end-caps at the position closest to the beam pipe [1]. These radiation levels strongly depend on the location inside the calorimeter. They decrease significantly towards central rapidity and with increasing depth inside the calorimeter. The preamplifiers of the hadronic end-cap calorimeter will be located at the circumference of the calorimeter wheels. At this position, at a radius of $\sim 2 \text{ m}$ from the beam line, integrated maximum radiation levels of 0.3 kGy and $0.3 \cdot 10^{14} \text{ n cm}^{-2}$ are expected for an operation period of 10 years at high luminosity.

The corresponding electronics must withstand these radiation levels with a minimal deterioration of its performance in terms of gain, speed and linearity and with a small acceptable increase of noise. In the framework of the RD33 project [2] current sensitive preamplifiers based on GaAs MESFETs with a gate length of $1 \mu\text{m}$ [3] have been developed. They can be considered as prototypes for the final preamplifiers which will be used in the hadronic end-cap calorimeter.

In order to address the radiation hardness question, the RD33 preamplifiers were exposed to an integrated neutron fluence of $9 \cdot 10^{14} \text{ n cm}^{-2}$ and to a γ dose of 31 kGy . The irradiation was performed at nuclear power reactors at the Joint Institute for Nuclear Research at Dubna. Parameters of the preamplifiers, like the transfer function, the rise time, the linearity and the equivalent noise current, were measured before and during the irradiation. After a brief description of the Dubna irradiation facilities and the measurement setup the results of these measurements are presented in the following.

2 Experimental Setup at the Dubna Reactors

The irradiation has been carried out at the pulsed neutron reactors [4] IBR-2 and IBR-30 at Dubna. The IBR-2 reactor has a working frequency of 5 Hz, a half-width of the reactor pulse of about $220 \mu\text{s}$ and a peak power in the pulse of about 1500 MW. Via 14 horizontal extraction channels the reactor IBR-2 can deliver a neutron flux up to $10^{12} \text{ n cm}^{-2}\text{s}^{-1}$ over areas up to $20 \times 40 \text{ cm}^2$. In addition to the neutrons, also γ radiation is produced in the nuclear reactions with maximal dose rates up to 10 Gy s^{-1} . The ratio between the neutron fluence and the γ dose can be varied by several orders of magnitude by using appropriate beam filters and absorbers.

For the present measurements a channel was used with a flux of fast neutrons of $\sim 10^{10} \text{ n cm}^{-2}\text{s}^{-1}$ and with a geometrical acceptance of $20 \times 40 \text{ cm}^2$. The setup of the experiment is presented schematically in Fig.1. During the whole period of irradiation the electronics was kept inside a cryostat at liquid nitrogen temperature. In order to suppress the γ radiation during the irradiation with neutrons, a 5 cm thick Pb filter was installed in front of the cryostat. In the case of γ irradiation this filter was replaced by a n/γ converter consisting of a paraffin moderator interleaved with cadmium foils. The activation of the

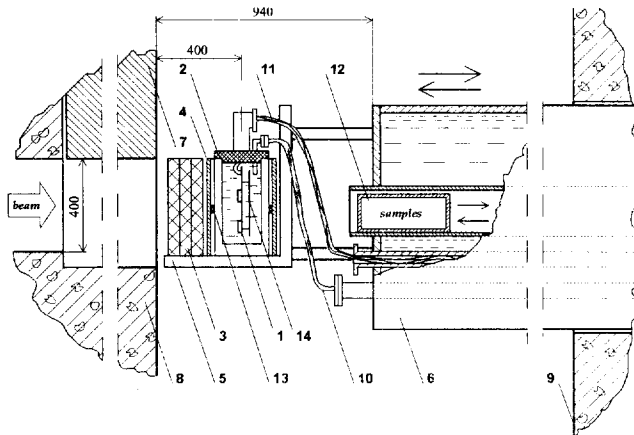
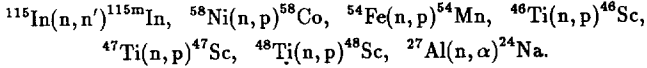


Figure 1: Schematic layout of the experimental setup: (1) motherboard with the electronics; (2) cryostat; (3) beam filter; (4) boron carbide layer; (5) support frame; (6) movable shielding platform; (7) beam shutter; (8) inner and (9) outer reactor shields; (10) cryogenic lines; (11) measurement cables; (12) tube for samples transporting; (13) neutron and γ dosimeters; (14) nickel foil.

equipment by thermal neutrons was reduced by a 5 mm thick layer of boron carbide (B_4C) surrounding the cryostat. A movable platform allowed to position the cryostat for the irradiation at a distance of 10 cm from a beam shutter in the space between an inner and outer reactor shield. During the experiment the cryostat was filled remotely with liquid nitrogen using special cryogenic lines. Additional tubes are available for measurement cables and for the transport of different samples of materials to the irradiation zone. The equipment for data taking was assembled in a counting room at a distance of about 15 m from the outer shielding wall. The measurement cables had a total length of 40 m. In order to monitor the dose rate, neutron and γ dosimeters were mounted temporarily around the cryostat in a special dedicated run at low reactor power. In addition, a large nickel foil covering the backside of the motherboard with the electronic chips was kept in the cryostat during the whole irradiation period. The induced activity in this foil was used for both the monitoring of the total reactor power and the measurement of the homogeneity of the neutron fluence. It has been found to be homogeneous within $\pm 5\%$ over the area of the electronics board.

3 Particle Fluences and Dose Rates

The standard methods of threshold detector activation were used to measure the kinetic energy spectrum and the absolute value of the neutron fluence. The spectrum was reconstructed by applying an unfolding procedure to the yield measurements of the following reactions:



The threshold values for these reactions are in the range between 0.4 and 6 MeV. The yields were determined from the measurements of the induced γ activity with GeLi detectors. Using this method the kinetic energy spectra of the neutrons from the reactor were measured for the two types of beam filters, as shown in Fig.2. The average kinetic energy of the neutrons was found to be ~ 1.5 MeV in the setup including the lead absorber. Since

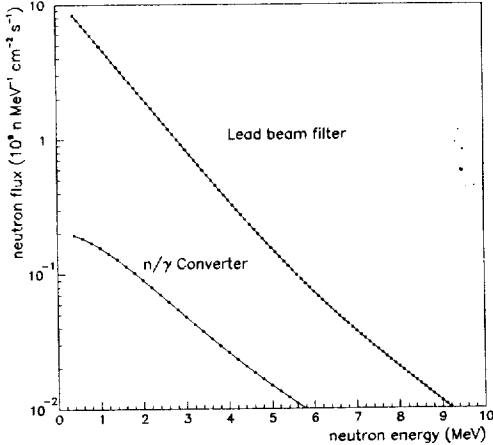


Figure 2: The kinetic energy spectra of the neutrons from reactor IBR-2 for two types of the beam filter.

the measurement of the spectrum was not possible below the lowest energy threshold of 0.4 MeV, the additional fluence from neutrons with energies below this value has been estimated to be $\sim 30\%$ using Monte Carlo calculations. It will be denoted as ϕ_{MC} in the following.

In order to compare the results obtained in different radiation hardness tests, the fluence values have been recalculated as effective values for neutrons with an equivalent energy of 1 MeV. The corresponding fluence value $\phi_{eff}(1 \text{ MeV})$ is given by:

$$\phi_{eff}(1\text{MeV}) = \int_{E_{\min}}^{E_{\max}} \phi_{meas}(E) \frac{D(E)}{D(1 \text{ MeV})} dE,$$

where $\phi_{meas}(E)$ is the measured neutron fluence and $D(E)$ is the energy dependent neutron kerma-factor¹ for atomic displacements in GaAs [5]. The effective neutron fluence has been obtained as

$$\phi_{eff}(1 \text{ MeV (GaAs)}) = 1.15 \cdot \phi_{meas}(0.4 - 11 \text{ MeV}) + 0.37 \cdot \phi_{MC}(0.1 - 0.4 \text{ MeV}).$$

¹kerma: kinetic energy released in matter

The second term takes into account the effective 1 MeV fluence from neutrons with an energy in the range between 0.1 and 0.4 MeV. The factor 0.37 results from the low kerma factors of low energy neutrons. The contributions from neutrons with energies below 0.1 MeV to the 1 MeV equivalent fluence was estimated to be below 5% of the total fluence and has been neglected. The uncertainty on the evaluated neutron fluences has been estimated to be at the level of $\pm 15\%$. All values quoted in the following correspond to effective fluences of neutrons with an energy of 1 MeV.

At the IBR-2 reactor a neutron flux of $(8.9 \pm 1.3) \cdot 10^9 \text{ n cm}^{-2} \text{ s}^{-1}$ was available for the neutron irradiation of the electronics. During a total irradiation time of 28 hours a total neutron fluence of $(9.0 \pm 1.4) \cdot 10^{14} \text{ n cm}^{-2}$ was collected in nine steps. The remaining total γ dose was measured to be at the level of $(1.4 \pm 0.2) \text{ kGy}$ at the end of the experiment by using thermo-luminescent dosimeters of the type TLD-700 [6].

The photon irradiation has been performed at the reactor IBR-30 which has the same operational principle as IBR-2. The half-width of the fast neutron pulse is about $4 \mu\text{s}$ and the flux of fast neutrons is $10^{11} \text{ n cm}^{-2} \text{ s}^{-1}$ near the reactor moderator surface. The reactor geometry allowed for a larger suppression of the neutron background compared to the IBR-2 reactor. In particular, the equipment could be protected from the backside against rescattered neutrons. The fluence of fast neutrons was attenuated by a combination of a paraffin moderator and a cadmium absorber, where neutrons were absorbed in n- γ reactions. The γ spectrum consists of three different components, the prompt photons from the nuclear reactions emitted during the reactor bursts, delayed photons emitted from the deexcitation of nuclei in between the bursts, and photons from the Cd (n- γ) reaction. The energy spectra of the primary and delayed photons have been measured previously [7]. Taking into account all components, the average photon energy was found to be in the range between 1.5 and 2.0 MeV. The γ -dose rate was measured to be 0.3 kGy/h . During the measurement period of about one week a total dose of $(31 \pm 3) \text{ kGy}$ was collected in seven steps. At the end of the irradiation the integrated underlying neutron fluence was measured to be $(0.66 \pm 0.13) \cdot 10^{14} \text{ n cm}^{-2}$.

4 Results on Radiation Hardness

In order to simulate the response of a liquid argon gap to the passage of a particle, triangular pulses from a pulse generator were sent into the GaAs preamplifiers. The signal output from the preamplifiers was fed into a shaper system [8] which allowed for the selection of the time constant τ of the shaper in the range between 10 ns and $10 \mu\text{s}$. The shaper output was sent into a digital scope which was read out by a computer system. Two GaAs preamplifier chips with five channels each were mounted onto the preamplifier board in the cryostat. Parallel to some amplifier channels, capacitors of 125 and 330 pF were mounted to simulate detector signal sources with different capacitances. The range between $C_d = 125 \text{ pF}$ and 330 pF is typical for the operation in the hadronic end-cap calorimeter of the ATLAS experiment. For all channels the transfer function, i.e. the output voltage as a function of the input current, the rise time (τ_p) of the pulse after the shaper and the equivalent noise current (ENI) were measured. All measurements were performed as a function of the shaping time.

4.1 Transfer Function and Rise Time

The transfer function was measured after each radiation step for ten different shaping times in the range between 10 ns and 10 μ s. This measurement monitors the gain stability of the preamplifiers during the irradiation. The results obtained for three channels with different detector capacitances are presented in Fig.3 for both neutron and γ irradiation.

Shown are the ratios of the transfer function values measured at each radiation step normalized to the ones measured before irradiation. The shaping time τ is given as a parameter on the plots. For stable operation no deviations from unity should occur. As can be seen from Fig.3a the measured deviations from 1 do not exceed 20% in the case of photon irradiation. However, larger deviations are found under neutron irradiation beyond integrated fluences of $\sim 3 \cdot 10^{14}$ n cm^{-2} . In particular for the channel with large capacitance a significant drop in the response is observed. It should be noted that the same behaviour is found for the other channels with the same capacitance values.

The DC voltage at the preamplifier output changed under irradiation as well. After a neutron fluence of $3 \cdot 10^{14}$ n cm^{-2} the DC voltage dropped by $\sim 25\%$ for all channels measured. Smaller changes in the DC voltage were observed under γ irradiation. The ratio of the measured voltage values to the one measured before irradiation are shown in Fig.4 as a function of the γ dose and the neutron fluence. Given the fact that the neutron background of $0.66 \cdot 10^{14}$ n cm^{-2} collected during the γ irradiation was relatively high, the deviations of the transfer function ratio from unity might also have been caused by the underlying neutrons.

In Fig.5 the measured rise time, defined as the time needed for the pulse to go from the 5% level to the peak, is shown as a function of the irradiation level for both photons and neutrons. Since the rise time is measured after the shaper, a convolution of the rise time of the preamplifier and the shaper response is measured. In the case of γ irradiation a very stable behaviour is found with essentially no increase of the measured rise time with increasing dose level. The effect is found to be much more severe under neutron irradiation, in particular for the channels with large detector capacitance. Beyond fluence values of $\sim 3 \cdot 10^{14}$ n cm^{-2} the rise time increases drastically. The increase is largest for small shaping times, where the rise time is dominated by the preamplifier response. For shaping times beyond ~ 100 ns the shaper response itself dominates which is not affected by the irradiation.

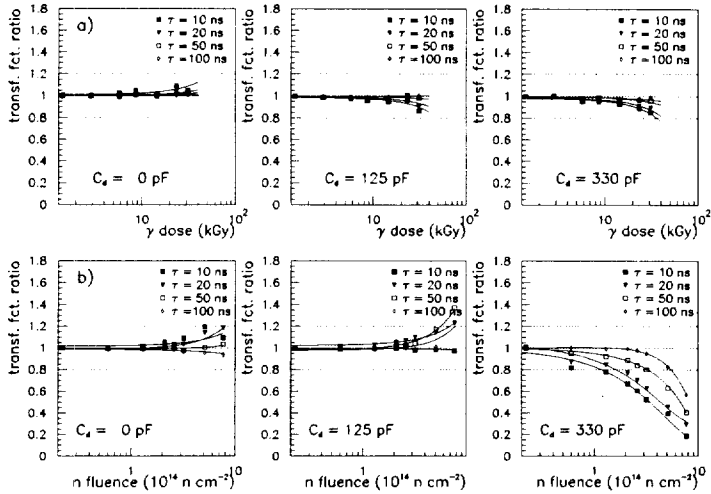


Figure 3: Ratio between the transfer function values measured after the various irradiation steps and the values measured before irradiation: (a) γ and (b) neutron irradiation. In each case three preamplifier channels with different detector capacitance are plotted for four different shaping times.

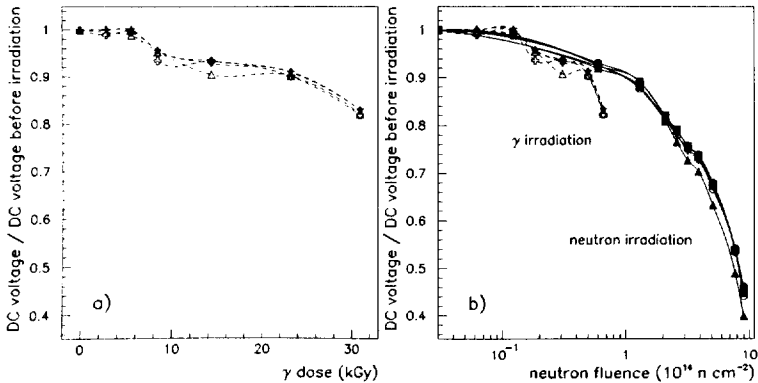


Figure 4: Ratio between the DC voltage measured after different irradiation steps and the one before irradiation as a function of the irradiation levels for all preamplifier channels used: (a) γ and (b) neutron irradiation. The values measured under γ -irradiation are also presented as a function of the underlying neutron fluence.

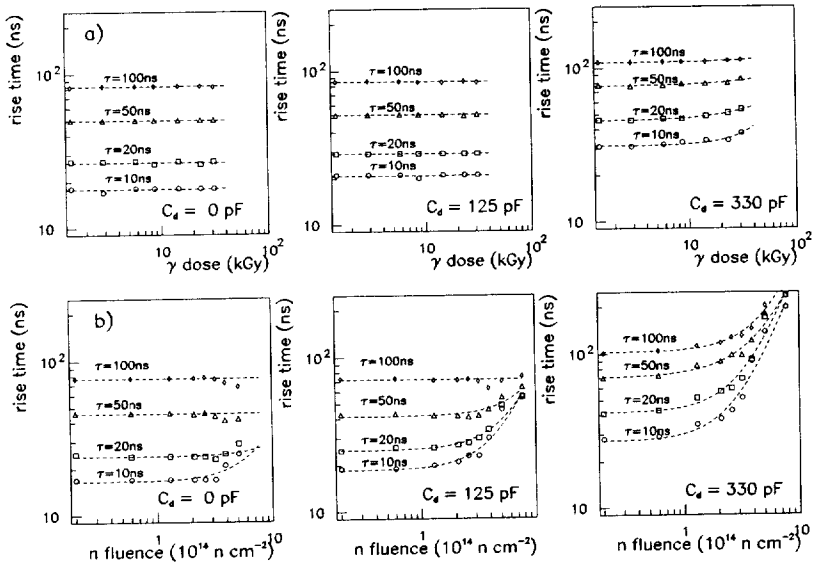


Figure 5: *The measured rise time of the pulse after the shaper as a function of irradiation levels: (a) γ and (b) neutron irradiation. The shaper time τ and the detector capacitance are given as parameters.*

4.2 Linearity

The linearity of the preamplifiers was measured for some channels by injecting triangular pulses in the input range from 0 to 2.5 mA. The results are presented in Fig.6 for a channel with a detector capacitance of 330 pF. Before irradiation a linear relation between the output voltage and the input current was observed. The same linear fit was repeated after the various irradiation steps. The fit was performed in the interval from 0 to 0.6 mA, which corresponds to the operational range for the RD33 preamplifiers in an LHC electromagnetic calorimeter. The slope and offset parameters obtained were compared to the ones determined before the irradiation. They have been found to be stable up to an integrated fluence of $\sim 4 \cdot 10^{14} \text{ n cm}^{-2}$. In the range from 4.0 to $7.7 \cdot 10^{14} \text{ n cm}^{-2}$ the slope parameter decreased by $\sim 20\%$ (see Fig.6b). Under γ irradiation no such degradation effects have been found. For all channels the slope parameters were stable up to the highest dose values accumulated.

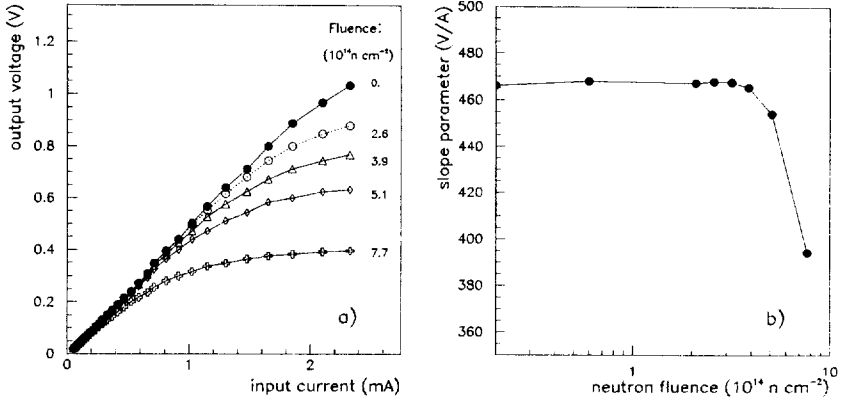


Figure 6: (a) The measured linearity for a preamplifier channel with a capacitance of 330 pF under neutron irradiation. (b) The slope parameters of a linear fit up to 0.6 mA as a function of the neutron fluence.

4.3 Equivalent Noise Current

From the measured rms spread of the shaper output voltage in the absence of any input signal, the equivalent input noise current (ENI) was computed by using the measured transfer function. The noise values measured before the irradiation are shown in Fig.7a as a function of the measured rise time. The data from all preamplifier channels are shown on the same plot. Three groups of points are clearly visible, corresponding to three different detector capacitance values. The measurements can be well described by the functional dependence

$$ENI = ENI(C_d, \tau_p) = \frac{\alpha}{\tau_p^{1.5}} \oplus \frac{\beta}{\tau_p^{0.5}}, \quad (1)$$

which is expected for a current sensitive amplifier. The fitted values for the parameter α are shown in Fig.7b. As expected, they scale with the detector capacitance. It must be noted that the experimental setup was sensitive to low frequency pickup noise, such that the noise measurements had to be limited to shaping times below 1 μ s. The dependence of the noise on the neutron fluence is shown in Fig.8a. The data are presented for three typical channels with different capacitances. An increase of the rise time measured for small shaping times is clearly visible when irradiated. For very high neutron fluences, exceeding $\sim 1 \cdot 10^{14}$ n cm⁻², an increase of the equivalent noise current becomes significant as well, in particular for long shaping times. Under γ irradiation, the equivalent noise starts rising already for relatively low radiation dose values. The increase of noise is also seen for short measured rise times, indicating that it is not limited to the low frequency part of the noise spectrum. The corresponding data are shown in Fig.8b.

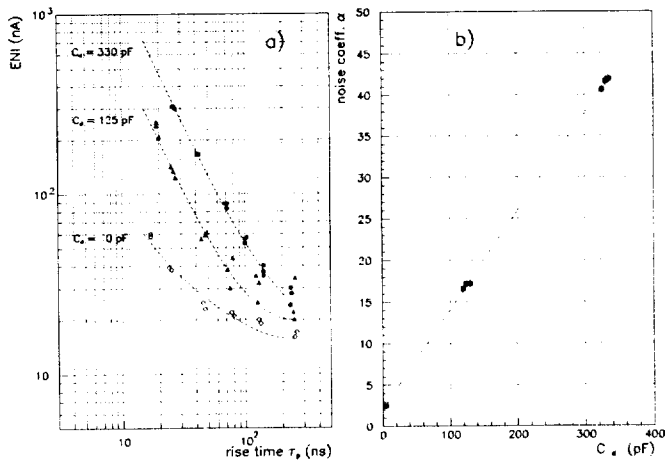


Figure 7: (a) The measured equivalent noise current before irradiation for all preamplifier channels. (b) The fitted values of the noise parameter α as defined in eq.(1) as a function of detector capacitance.

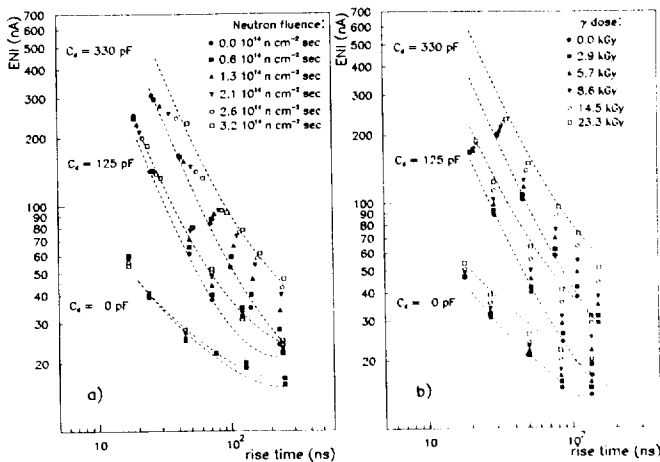


Figure 8: The measured equivalent noise currents during irradiation for three preamplifier channels with different capacitances C_4 : (a) neutron, (b) γ irradiation.

The increase of noise, normalized to the values measured before irradiation, is shown for all preamplifier channels in Fig.9. The results are given for two fixed values of the measured rise time, chosen to be 40 and 100 ns. As indicated above, the increase of noise is small under neutron irradiation for small shaping times up to fluence values in the order of $\sim 1 - 2 \cdot 10^{14}$ n cm⁻². This is found to be true for all channels independent of the detector capacitance. Under photon irradiation the noise increases continuously. For the channels with a capacitance of 125 pF an increase in the range between 15 and 30% is seen after a collected dose of 20 kGy at a rise time of 40 ns. It must be noted that the observed spread between the various channels is large and that the small number of irradiated preamplifier channels precludes more detailed conclusions.

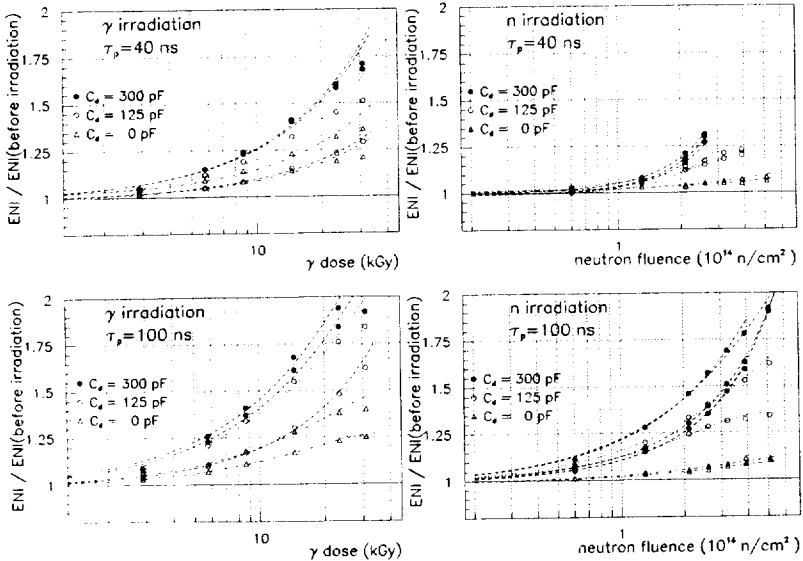


Figure 9: The equivalent noise current (ENI) measured during irradiation normalized to the value measured before irradiation. The data are shown for all preamplifier channels as a function of the irradiation levels for both neutron and γ irradiation and for two different values of the measured rise time, chosen to be 40 and 100 ns. Note that for neutron fluences exceeding $3 \cdot 10^{14}$ n cm⁻² the measured rise time for all channels with $C_d = 330$ pF is larger than 40 ns and no data points are included in the figure.

5 Conclusions

The GaAs preamplifiers developed in the framework of the RD33 project show a stable performance in terms of transfer function, rise time and linearity up to high neutron fluences of $\sim 3 \cdot 10^{14}$ n cm⁻². For neutron fluences exceeding this value clear deteriorations in the preamplifier performance have been observed. In particular for the channels with large detector capacitance a decreased response function together with an increased rise time have been measured. Under γ irradiation no damage of the performance has been seen up to 31 kGy, the maximum γ dose accumulated. The equivalent noise current has been found to increase under irradiation for both neutrons and photons. Under neutron irradiation the increase is small for short shaping times up to fluence values of $\sim 3 \cdot 10^{14}$ n cm⁻². Under photon irradiation a continuous increase is observed, starting already at low dose rates.

For the radiation levels expected after 10 years of operation at high luminosity in the hadronic end-cap calorimeters of the ATLAS experiment (0.3 kGy and $0.3 \cdot 10^{14}$ n cm⁻²) both the increase of the equivalent noise current and the increase of the rise time are found to be small. Therefore, an application of the proposed electronics looks uncritical from the radiation hardness point of view. However, it should be noted that for an application of the electronics chips inside the electromagnetic end-cap calorimeter, as proposed in the RD33 project [9], a severe damage would occur for preamplifiers in the region of large pseudorapidity, $|\eta| > 2.0$. Since in the proposed solution the preamplifiers would have been located in the liquid argon close to the readout pads, they would have been exposed to a neutron fluence of $3.0 \cdot 10^{15}$ n cm⁻² and a γ dose of 100 kGy after 10 years of LHC operation in the pseudorapidity region $|\eta| > 2.0$.

It should also be mentioned that the present results were obtained using high neutron fluences and γ dose rates to evaluate on the time scale of a week the radiation damage after 10 years of operation at LHC. The conclusions might therefore change if considerable dose rate dependent effects or annealing effects exist.

The present results are in good agreement with previous measurements performed at different institutes [10].

Acknowledgements

The continuous help and support of the engineers and technicians of the JINR Dubna reactor group and the MPI Munich is acknowledged. Financial support from the German Bundesministerium für Bildung, Wissenschaft, Forschung und Technologie, under contract number 6MP13I, is acknowledged. We also wish to thank D.V. Camin, C. de la Taille and N. Fedyakin for stimulating and fruitful discussions.

References

- [1] ATLAS Collaboration, Technical Proposal, CERN/LHCC/94-43 (1994);
M. Shupe, private communication.
- [2] RD33 Collaboration, C. Berger et al., Nucl. Instr. & Methods, **A357** (1995) 333;
RD33 Collaboration, W. Braunschweig et al., Nucl. Instr. & Methods, **A378** (1996)
479.
- [3] QEDA process of the foundry TRIQUINT.
- [4] E. Shabalin, Fast pulsed and burst reactors, Pergamon Press Ltd., Oxford, (1979).
- [5] A.M. Ougouag et al., IEEE Trans. Nucl. Sci. **NS-37** (1990) 2219.
- [6] Harshaw Chemical Co., Cleveland, Ohio 44106, USA.
- [7] V.A. Khitrov and Pack Hong-Cher, JINR Internal Report, Dubna (1974).
- [8] C. de la Taille, Orsay preprint, LAL/RT 92-10 (1992).
- [9] RD33 Collaboration, C. Berger et al., CERN DRDC Proposal, CERN/DRDC 93-02
(1993).
- [10] D.V. Camin (RD3 Collaboration), Proc. IV Int. Conf. on Calorimetry in HEP, World
Scientific, (1994) 618;
M. Citterio, V. Radeka and S. Rescia, Proc. V IEEE Trans. Nucl. Science Vol.42,
No.6 (1995) 2266.

Received by Publishing Department
on November 5, 1996.

Чеплаков А. и др.

E13-96-358

Радиационная стойкость GaAs предусилителей
для жидкоаргоновой калориметрии на LHC

Предусилители, созданные на базе GaAs технологии, предназначены для считывания информации с торцевого жидкоаргонового адронного калориметра в эксперименте АТЛАС на LHC. Погруженные в жидкий аргон предусилители должны сохранить работоспособность в тяжелых радиационных условиях во время работы коллайдера LHC при наивысшей его светимости и в течение всего эксперимента. Аналогичные предложенным предусилители были подвергнуты воздействию быстрых нейтронов и гамма-квантов до высокого уровня флюенса и гамма-дозы. Существенного ухудшения рабочих характеристик предусилителей вплоть до уровня нейтронного флюенса около $3 \cdot 10^{14}$ н см⁻² и наивысшей гамма-дозы 31 Gy не наблюдалось. Только незначительное увеличение эквивалентного шумового тока было отмечено также при достижении радиационного уровня, ожидаемого в эксперименте АТЛАС.

Работа выполнена в Лаборатории сверхвысоких энергий и в Лаборатории нейтронной физики им.И.М.Франка ОИЯИ.

Препринт Объединенного института ядерных исследований. Дубна, 1996

Cheplakov A. et al.

E13-96-358

Radiation Hardness of GaAs Preamplifiers
for Liquid Argon Calorimetry at LHC

Cold preamplifiers, designed in GaAs technology, are foreseen in the readout chain of the hadronic liquid argon end-cap calorimeter of the ATLAS experiment at LHC. The preamplifiers immersed in the liquid argon must withstand the hostile radiation environment during the operation of the LHC machine at the highest luminosities for the whole expected lifetime of the experiment. Preamplifiers, with a layout similar to the ones proposed, have been exposed to a high fluence of fast neutrons and to a high dose of γ radiation. No significant deterioration of the performance has been observed for a neutron fluence up to $\sim 3 \cdot 10^{14}$ н см⁻² and up to 31 kGy, the highest γ dose collected. Also only a moderate increase of the equivalent noise current has been seen for the radiation levels relevant for the operation in the ATLAS experiment.

The investigation has been performed at the Laboratory of Particle Physics and at the Frank Laboratory of Neutron Physics, JINR.

Preprint of the Joint Institute for Nuclear Research. Dubna, 1996

Макет Т.Е.Попеко

Подписано в печать 25.12.96
Формат 60 × 90/16. Офсетная печать. Уч.-изд.листов 1,43
Тираж 380. Заказ 49607. Цена 1716 р.

Издательский отдел Объединенного института ядерных исследований
Дубна Московской области